

We investigate the minimal streamer model, i.e., a "fluid approximation" with local field-dependent impact ionization reaction in a non-attaching gas like argon or nitrogen [1,6{11]. In detail, the dynamics is as follows:

- (i) an impact ionization reaction in local field approximation: free electrons and positive ions are generated by impact of accelerated electrons on neutral molecules $\partial n_e + r_R = \partial n_i + r_R - j_e E n_e j_0$ ($\mathcal{E} j = E_0$); $n_{e,i}$ and $j_{e,i}$ are particle densities or currents of electrons or ions, respectively, and E is the electric field; in all numerical work, we use the Townsend approximation ($\mathcal{E} j = E_0$) = $\exp(\int E_0 = \mathcal{E} j)$ for the effective cross-section.
- (ii) drift and diffusion of the charged particles in the local electric field $j_e = -e E n_e - D_e r_R n_e$, where in anode-directed streamers the mobility of the ions actually can be neglected because it is more than two orders of magnitude smaller than the mobility of the electrons, so $j_i = 0$,
- (iii) the modification of the externally applied electric field through the space charges of the particles according to the Poisson equation $r_R (E = e(n_i - n_e)) = 0$. It is this coupling between space charges and electric field which makes the problem nonlinear.

The natural units of the model are given by the ionization length $R_0 = \lambda_0^{-1}$, the characteristic impact ionization field E_0 , and the electron mobility μ_e determining the velocity $v_0 = \mu_e E_0$ and the time scale $\tau_0 = R_0/v_0$. Hence we introduce the dimensionless coordinates [11] $r = R/R_0$ and $t = t/\tau_0$, the dimensionless field $E = E/E_0$, the dimensionless electron and ion particle densities $n_e = n_e/n_0$ and $n_i = n_i/n_0$ with $n_0 = \lambda_0 E_0 = (e R_0)$, and the dimensionless diffusion constant $D = D_e/(R_0 v_0)$. After this rescaling, the model has the form:

$$\partial_t n_e - r (E + D r) = f(\mathcal{E} j); \quad (1)$$

$$\partial_t n_i = f(\mathcal{E} j); \quad (2)$$

$$r = r - E; E = r; \quad (3)$$

$$f(\mathcal{E} j) = \mathcal{E} j - \mathcal{E} j^2 = \mathcal{E} j e^{1-\mathcal{E} j} \text{ in sim. } : (4)$$

In the simulations presented here, a planar cathode is located at $z = 0$ and a planar anode at $z = 2000$. The stationary potential difference between the electrodes $\Delta V = 1000$ corresponds to a uniform background field $E = 0.5 \text{ eV/cm}$ in the z direction. For nitrogen under normal conditions with effective parameters as in [9,10], this corresponds to an electrode distance of 5 mm and a potential difference of 50 kV . The unit of time τ_0 is 3 ps , and the unit of field E_0 is 200 kV/cm . We used $D = 0.1$ which is appropriate for nitrogen, and we assumed cylindrical symmetry of the streamer. The radial coordinate extends from the origin up to $r = 2000$ to avoid lateral boundary effects on the field configuration. As initial condition, we used an electrically neutral Gaussian ionization seed on the cathode

$$n(r; z; t = 0) = n_i(r; z; t = 0) = 10^{-6} e^{-(z^2 + r^2)/100^2} : (5)$$

The parameters of our numerical experiment are essentially the same as in the earlier simulations of Vitello et al. [10], except that our background electric field is twice as high; the earlier work had 25 kV applied over a gap of 5 mm . This corresponded to a dimensionless background field of 0.25 , and branching was not observed.

In Fig. 1 we show the electron density levels at four time steps of the evolution in the higher background field of 0.5 . We observe that at time $t = 420$, the streamer develops instabilities at the tip. At time $t = 450$, these instabilities have grown out into separate fingers. Because of the imposed cylindrical geometry, the further evolution after branching ceases to be physical. On the other hand, the main effect of the unphysical symmetry constraint is to suppress all linear instability modes that are not cylindrically symmetric. Hence in a fully 3D system, the instability will develop even earlier than here.

Further simulations show: (a) branching does not occur in a system of the same size in the lower background field of 0.25 , in agreement with [10]. (b) Branching is not due to the proximity of the anode, since in a system with twice the electrode distance (with the anode at $z = 4000$) and with twice the potential difference ($\Delta V = 2000$) so with the same background field, the streamer branches in about the same way after about the same time and travel distance. (c) However, branching does somewhat depend on the numerical discretization. In fact, numerical noise due to the discreteness of the spatio-temporal grid is the only noise present in our mean field model (1) - (5). It substitutes the physical noise caused by the discreteness of the individual charge carriers. A wider numerical mesh leads to a higher effective noise level; and in agreement with this reasoning, in the simulation the branching then develops somewhat earlier. (d) Occasionally, we observe a different tip splitting mode. In Fig. 1 at time $t = 450$, the finger on the axis develops the strongest with n_e exceeding 6 , while in the fingers off the axis, n_e stays below 3 . In the other branching mode, the first finger off the axis outruns the finger on the axis.

Before we discuss the physical nature of the instability, we explain our numerical approach: we used uniform space-time grids with a spatial mesh of 1000×1000 . The spatial discretization is based on local mass balances. The diffusive fluxes are approximated in standard fashion with second order accuracy. For the convective fluxes a third order upwind-biased formula was chosen to reduce the numerical oscillations that are common with second order central fluxes. Time stepping is based on an explicit linear 2-step method, where at each time step the Poisson equation is solved by the FISHPACK routine. References for these procedures can be found in [13].

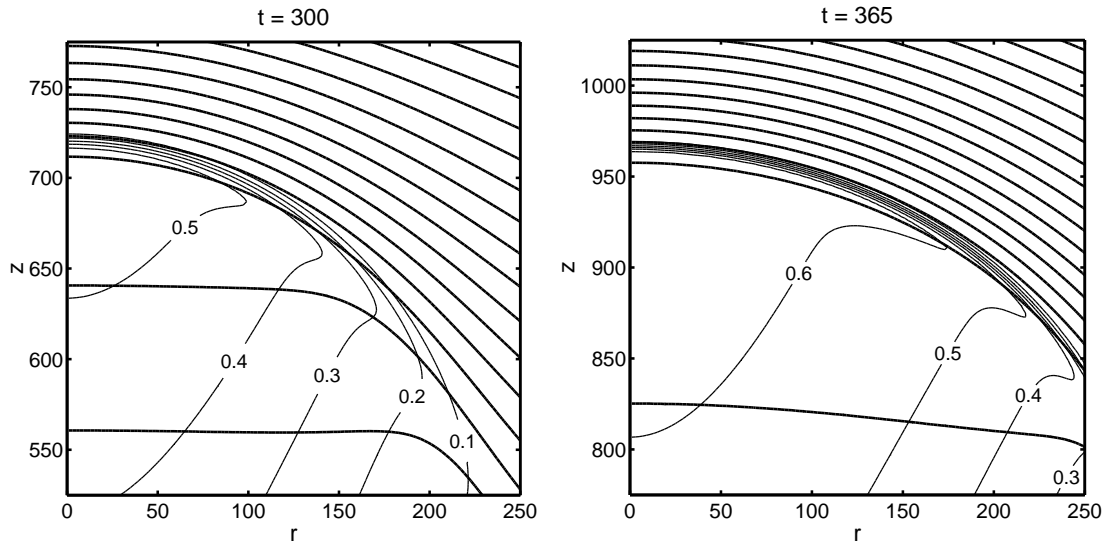


FIG. 2. A zoom into the head of the streamer from Fig. 1 at the first two time steps. The aspect ratio is equal and the axis scaling identical at both times. The thin lines are the levels of equal electron density as in Fig. 1. The thick lines are electrical equipotential lines in steps of $\phi = 12$.

To understand now why and at which stage the streamer becomes susceptible to noise and develops a tip splitting instability, in Fig. 2, we zoom into the streamer head. Shown are the first two time steps from Fig. 1 with the electron density levels again as thin lines, and additionally with the equipotential lines as thick lines. One observes that during the temporal evolution prior to branching, both the curvature and the thickness of the ionization front decrease. So the width of the front becomes much smaller than its radius of curvature, and an interface approximation becomes increasingly justified. The electric field inside the streamer head also decreases, so that the ionization front more and more coincides with an equipotential surface. In summary, the ionization front evolves towards a weakly curved and almost equipotential moving ionization boundary. At the same time, the electric field immediately ahead of the streamer increases.

We argue now that a transient stage of an approximately equipotential and weakly curved ionization boundary leads to tip splitting. Conversely, we argue that tip splitting in the lower background field of 0.25 is not observed within the presently and previously [10] investigated gap lengths because the transient stage of Fig. 2 is not reached before the streamer reaches the anode.

In fact, the streamer in Fig. 2 approaches the limit of "ideal conductivity": the conducting body has constant σ , while in the non-ionized region $\sigma = 0$ due to the absence of space charges. The boundary between the two regions moves approximately with the drift velocity v_f / r or with the diffusion corrected velocity $v_f / r \sqrt{1 + 2 \frac{D_p}{D} (\nabla_r^2 j) = \nabla_r^2 j}$ [11]. Our simulations are the first numerical evidence that the "ideal

conductivity" limit can be approached within our model.

This limit of ideally conducting streamers in an electric field that becomes uniform far ahead of the front was studied by Firsov [6]. He realized that uniformly propagating paraboloids of arbitrary radius of curvature are solutions of this problem. He did not realize that his paraboloids are mathematically equivalent to the Ivantsov paraboloids [12] of dendritic growth found earlier. The uniformly propagating Ivantsov paraboloids in the early 80's were identified as dynamically unstable. This is generally the case for such so-called Laplacian growth problems without a regularization mechanism. Since ideally conducting streamers also pose such a Laplacian growth problem [11], the dynamical instability of the structure shown in Fig. 2 can be expected, and it actually occurs as can be seen in Fig. 1. This explains qualitatively why tip splitting occurs.

For a quantitative analysis, a system specific regularization mechanism has to be found [11,12]. Its identification is intricate because negative streamer fronts are so-called pulled fronts whose dynamics is dominated by the leading edge rather than the nonlinear interior of the front [14]. Therefore standard methods like the perturbative derivation of a moving boundary approximation for the model (1)-(4) does not work [15]. (Pulling also implies that standard numerical methods with adaptive grids are inefficient.) However, the ionization front has two intrinsic length scales, a diffusion length and an electric screening length. We therefore explore the approximation of $D = 0$. It is smooth for the velocity of negative fronts [11] and eliminates the leading edge, and hence suppresses the pulled nature of the front. Rather the front becomes a shock front for the electron density, while the intrinsic length scale of the electric screening layer

behind the shock remains.

As a first step to understand the short wavelength regularization of perturbations due to this screening length, we have investigated the transversal instability modes of a planar ionization front in the limit $D = 0$ in a field that approaches the uniform limit $E = E_1 e_z$ far ahead of the front. The planar unperturbed front propagates with velocity $v = E_1$, which equals the drift velocity of the electrons precisely at the shock front. The implicit analytical front solution can be found in [11]. In a moving frame $z = z - vt$, we denote it by $\phi_0(z)$; $\phi_1(z)$; $\phi_2(z)$. The Fourier components $\tilde{\phi}_k$; $\tilde{\phi}_k$; $\tilde{\phi}_k$ of a transversal linear perturbation are defined through

$$\phi = \phi_0(z) + \int dk \tilde{\phi}_k(z) e^{ikx + st} + \dots \text{ etc.} \quad (6)$$

For the derivation of the boundary conditions on the shock front, it is more convenient to write a single Fourier component as $\phi = \phi_0 e^{ikx + st} + \phi_k(z) e^{ikx + st} + \dots$. With this ansatz and the auxiliary field $\phi_k = \phi_k$, the Fourier components solve the inhomogeneous equation

$$\begin{pmatrix} 0 & 1 & 0 & 1 & 0 \\ \partial_z & k & C & k & C \\ \partial_z & k & A & k & C \\ \partial_z & k & & k & \end{pmatrix} M_{s;k} \begin{pmatrix} \phi_0 \\ \phi_k \\ \phi_k \\ \phi_k \end{pmatrix} = \begin{pmatrix} s \phi_0 = (v + E_0) \phi_0 \\ s \phi_0 = v \phi_0 \\ E_0 k^2 \phi_0 \\ 0 \end{pmatrix} \quad (7)$$

$$M_{s;k} = \begin{pmatrix} 0 & 1 & 0 & 1 \\ \frac{s+2v-E_0}{v+E_0} \frac{f(E_0)}{v} & \frac{0}{s-v} & \frac{0}{v+E_0} & \frac{0}{v+E_0} \\ \frac{0}{f(E_0)=v} & 1 & 0 & 0 \\ 0 & 0 & 1 & 0 \end{pmatrix} \begin{pmatrix} \phi_0 \\ \phi_k \\ \phi_k \\ \phi_k \end{pmatrix} :$$

The boundary conditions at the shock $z = 0$ can be obtained from the analytical solution in the non-ionized area, and from the boundedness of the charge densities:

$$\begin{pmatrix} 0 & 1 & 0 & 1 \\ \partial_z & k & C & k & C \\ \partial_z & k & A & k & C \\ \partial_z & k & & k & \end{pmatrix} \begin{pmatrix} \phi_0 \\ \phi_k \\ \phi_k \\ \phi_k \end{pmatrix} = \begin{pmatrix} f^0(v) = (1 + s = f(v)) \phi_0 \\ 0 \\ 1 \\ (vk - s) = (sk) \end{pmatrix} \quad (8)$$

The other boundary conditions are obtained by imposing that at $z \rightarrow -\infty$ the electric field decays and the densities become constant.

These equations together with the boundary conditions define an eigenvalue problem for $s = s(k; v)$ with $v = E_1$. It can be solved numerically by shooting from $s = 0$ towards $s = 1$. In agreement with analytical limits | details will be given elsewhere |, we find

$$s(k) = \begin{cases} E_1 j k & \text{for } k > (E_1)^{-1/2} \\ E_1 j & \text{for } k < (E_1)^{-1/2} \end{cases} \quad (9)$$

This means that the electric screening length $l = (E_1)^{-1/2}$ does regularize the instability of short wavelength perturbations from linear growth in k to the saturation value $s(k) = E_1 j$ ($E_1)^{-1/2}$). A small positive growth rate remains, but the analytical derivation of (9) hints to the

unconventional possibility that sufficiently curved fronts actually are stable to short wavelength perturbations. This question is presently under investigation. If true, it would identify a most unstable wave length determining the width of the fingers that emerge after tip splitting.

In conclusion, we have presented numerical evidence that anode-directed streamers in a sufficiently strong, but uniform field can branch spontaneously even in a fully deterministic fluid model. We have argued that this happens when the streamer approaches the limit of ideal conductivity. We have established a qualitative mathematical analogy with tip splitting of viscous fingers through the concept of Laplacian growth, and we have analytically demonstrated that the electric screening length leads to an unconventional regularization. This opens the way to future quantitative analytical progress.

Acknowledgement: M.A. was supported by the EU-network "Patterns, Noise, and Chaos" and U.E. partially by the Dutch Science Foundation NWO.

New address: Universidad Rey Juan Carlos, Escuela Superior de Ciencias Exp. y Tecnología, c. Tulipán s/n, 28933 Móstoles, Madrid, Spain

[1] Y.P. Raizer, Gas Discharge Physics (Springer, Berlin 1991).
 [2] E.M. van Vekhuizen (ed.): Electrical discharges for environmental purposes: fundamentals and applications (NOVA Science Publishers, New York 1999).
 [3] A.A. Kulikovskiy, J. Phys. D: Appl. Phys. 33, 1514 (2000); and Phys. Rev. E 57, 7066 (1998).
 [4] L. Niemeyer, L. Pietronero, H.J. Wiesenmann, Phys. Rev. Lett. 52, 1033 (1984); A.D.O. Bawagan, Chem. Phys. Lett. 281-325 (1997).
 [5] H. Raether: Z. Phys. 112, 464 (1939) (in German).
 [6] E.D. Lozansky and O.B. Firsov, J. Phys. D: Appl. Phys. 6, 976 (1973).
 [7] M.I. Dyakonov, V.Y. Kachorovskii: Sov. Phys. JETP 67, 1049 (1988); and Sov. Phys. JETP 68, 1070 (1989).
 [8] E.M. Bazelyan, Yu.P. Raizer, Spark Discharges (CRS Press, New York, 1998); Yu.P. Raizer, A.N. Sinaikov, Plasma Phys. Rep. 24, 700 (1998).
 [9] S.K. Dhal and P.F. Williams, Phys. Rev. A 31, 1219 (1985) and J. Appl. Phys. 62, 4696 (1987).
 [10] P.A. Vitello, B.M. Penetrante, and J.N. Bardsley, Phys. Rev. E 49, 5574 (1994).
 [11] U. Ebert, W. van Saarloos and C. Caroli, Phys. Rev. Lett. 77, 4178 (1996); and Phys. Rev. E 55, 1530 (1997).
 [12] For a review and a collection of original articles, see P. Pelce: Dynamics of Curved Fronts (Academic Press, San Diego 1988).
 [13] P. Wesseling, Principles of Computational Fluid Dynamics, Springer Series in Comp. Math. 29 (Berlin 2001).
 [14] U. Ebert and W. van Saarloos, Phys. Rev. Lett. 80, 1650 (1998); and Physica D 146, 1 (1999) (2000).
 [15] U. Ebert, W. van Saarloos, Phys. Rep. 337, 139 (2000).